3D antidunes preserved on fine-grained sand bed in an experimental flume: Genetic conditions and their sedimentary structures

M. Yokokawa
Osaka Institute of Technology, Hirakata, Osaka, Japan

K. Hasegawa & S. Kanbayashi
Hokkaido University, Sapporo, Hokkaido, Japan

N. Endo
Kanazawa University, Kanazawa, Ishikawa, Japan

ABSTRACT: Antidunes and their sedimentary structures can be useful in reconstructing paleo-hydraulic condition, especially for large discharge events. However, 3D antidunes in sand-sized sediments have not yet been studied extensively as compared to either 2D antidunes or in gravel-sized sediments. In this study, we applied genetic conditions of 3D gravel step-pool topographies to sand beds, and proved that 3D mound-like antidune configurations and internal sedimentary structures could be preserved. The genetic condition is expressed as the relationship between the bed slope and the water discharge. Thus this result indicates that the existence of 3D antidune configurations can help in the more precise reconstruction of paleo-hydraulic parameters such as flow-depth and water discharge as compared to previous methods. Internal sedimentary structures were characterized by shallow lens-like structures whose bases are erosional. Although gently dipping concave-upward lamination occurs dominantly, convex-upward lamination is occasionally observed as well. It appears that the geometry of lenticular laminasets can be used to estimate the antidune geometry and thus it would still be possible to estimate the paleo-hydraulic parameters even if only the sedimentary structures of 3D antidunes are left.

1 INTRODUCTION

Antidunes are bedforms generated by unidirectional flows in the upper flow regime. Previous flume experiments have revealed that when the flow velocity increases, antidunes are formed next to the upper-stage plane bed formations in sand-sized sediments, and next to dune formations in gravel-sized sediments (e.g., Boguchwal & Southard, 1990).

Despite their abundance in rock records, it has been pointed out that the sedimentary structures of the interpreted upper flow regime origin might have remained unnoticed (Fielding, 2006). Bedforms and sedimentary structures originating from the upper flow regime are often formed by catastrophic floods; therefore, understanding their characteristics and genetic conditions will be useful for reconstructing the environmental changes induced by such catastrophic events. This does not apply only to the Earth's surface; it will also be very useful for estimating the discharge of channels on other planets such as Mars through image analysis (e.g., Burr et al., 2004).

There are two types of antidune geometries, namely, 2D and 3D. 2D antidunes have continuous crest lines transverse to the flow, while 3D antidunes have discontinuous crests or mound shapes. Both 2D and 3D gravel antidunes, including "putative" ones, have been reported from modern and Quaternary river (flood) and glacial outwash deposits (e.g., Shaw & Kellerhals, 1977; Alexander & Fielding, 1997; Carling & Breakspear, 2007). On the other hand, in the case of sand-sized sediments, 2D antidunes have been reported from modern and ancient rivers (e.g., Langford & Bracken), washover-fans (e.g., Barwis & Hayes, 1985), beaches (Augustinus, 1980), and volcanic-ash-base-surges (e.g., Schmincke et al., 1973; also see Allen's (1982) comprehensive review of other examples). However, fairly limited 3D antidunes have been found in sandy beds, and all of these have been reported from ancient rock records, i.e., fluvial sandstone (Rust & Gibling, 1990; Masuda et al., 1993; Collinson et al., 2006) and turbidites (Prave & Duke, 1990). These antidunes have been noticed because they exhibit internal sedimentary structures that are identical to the hummocky beds that are observed in shallow marine deposits that are affected by waves.

There have been a good number of theoretical and experimental works on antidune formation (see the review of Allen, 1982; Carling & Shvidchenko, 2002). Kennedy's works (Kennedy, 1961, 1963, 1969) can be considered to be the most well known and cited ones. Kennedy (1991, 1963) showed the formative condition of antidunes in terms of the relationship between the Froude number and the wave number. Furthermore, Kennedy (1961, 1963) called 3D antidunes “short-crested antidunes,” and showed that they appear at Froude numbers greater than $\sqrt{1/kh}$, where, k is wave number and h is the average water depth, whereas 2D antidunes form at lower Froude numbers (Kennedy, 1963). However, the formative condition of sandy 3D antidunes has hardly been studied experimentally after Kennedy's (1963) studies.

On the other hand, transverse ribs, which are cobble and boulder ridges oriented transverse to the flow, and stone cells, which are cellular networks of stones, are observed in the outwash fans and they are considered to be relict antidune bedforms (e.g., Gustavson, 1974). In mountainous rivers, it has been known that there exist small (wavelength: 2–20 m) channel units called “ribs” and “step-pools” (e.g., Hasegawa et al., 1990). A “rib” is a step-like topography in which gravel forms ridges transverse to the flow, whereas gravel forms circles in a “step-pool.” Whittaker & Jaeggi (1982) and Ashida et al. (1984) revealed that ribs are formed by antidunes and sorting effects. Hasegawa & Kanbayashi (1996) showed that step-pools are generated due to the interaction of antidunes and 3D water surface waves (diagonal cross-waves) on a supercritical flow. When the wavelengths of the antidunes and water surface waves coincide, the 2D undulation of the antidunes gradually becomes 3D and then, the surface waves begin to be amplified. They developed equations that represent the genetic conditions of step-pools and verified them experimentally.

In this study, we applied Hasegawa & Kanbayashi's (1996) genetic conditions for 3D gravel step-pools to fine sand, and examined the resultant bedforms formed in the flume. The genetic condition of 3D antidunes in fine sand is presented in terms of the relationship between the water discharge per unit width and the bed slope, and the internal sedimentary structures were also observed in detail.

2. GENETIC CONDITIONS FOR 2D AND 3D ANTIDUNES

2.1. General conditions for antidune formation

Potential flow analyses, developed by Anderson (1953) and Kennedy (1963), give the condition for antidune formation as

$$Fr > Fr_1 \tag{1}$$

Here, Fr is the Froude number and it is defined as:

$$Fr = U/\sqrt{gh}$$

where U denotes the depth-averaged velocity; h, the average water depth; and g, the acceleration due to gravity.

Fr_1 is expressed as:

$$Fr_1 = \sqrt{\tanh(kh)/kh} \tag{2}$$

where k denotes the wave number of the bed undulations, and it is given by the relationship $k = 2\pi/L_b$, where L_b denotes the bedform wavelength.

Moreover,

$Fr > Fr_1$ and $Fr < Fr_u$,

where

$$Fr_u = \sqrt{1/(kh)\tanh(kh)} \tag{3}$$

and with larger values of kh (approx. $kh \geq 1$), the antidunes migrate downstream (e.g., Carling & Shvidchenko, 2002; Parker, 2004).

In addition, Kennedy (1963) reported that in the area expressed as

$Fr > Fr_m$

where

$$Fr_m = \sqrt{\frac{1}{kh}}, \tag{4}$$

2D antidunes (long-crested waves) are not a possible configuration; instead, short-crested waves (3D antidunes) occur.

On the other hand, Kennedy (1961; after Foley, 1977) found that the wavelengths of stationary waves and antidunes are related to the mean flow velocity by the equation:

$$U = \sqrt{\frac{gL_b}{2\pi}} \tag{5}$$

Furthermore, Kennedy (1961; after Foley, 1977) derived a velocity-wavelength relationship for 3D stationary waves from the inviscid flow theory and found a qualitative experimental agreement in the form:

$$U = \sqrt{\frac{gL_b}{2\pi}} \cdot \left[1 + \left(\frac{L_b}{L_t}\right)^2\right]^{\frac{1}{4}} \tag{6}$$

where L_t denotes the transverse wavelength of the 3D antidune.

2.2. Genetic conditions of step-pools

Hasegawa & Kanbayashi (1996) showed that step-pools are generated due to the interaction of antidunes and 3D water surface waves (diagonal cross-waves) in a supercritical flow. When the wavelengths of the antidunes and water surface waves coincide, the 2D undulation of the antidunes gradually becomes 3D and then, the surface waves begin to be amplified. When the 2D antidunes and surface diagonal waves have different wavelengths, they cancel out. Therefore, Hasegawa & Kanbayashi (1996) analyzed the conditions in which the wavelengths of both the 2D antidunes and the water surface diagonal cross-waves are the same.

First, to express the relationship between the wavelength of the antidunes and the Froude number, Hasegawa & Kanbayashi (1996) used the equation below based on Hayashi (1970)'s work because their field data agreed with this equation:

$$Fr^2 = \frac{\coth(kh)}{kh} \approx \frac{1}{(kh)^2} + \frac{1}{3}. \tag{7}$$

The relationship between the Froude number and the water surface waves (diagonal cross-waves) is expressed as:

$$Fr^2 = \frac{\beta h}{(kh)^2}\tanh(\beta h) \approx \frac{\alpha\beta h}{(kh)^2} \tag{8}$$

$\alpha = 0.83,$

$\beta h = \sqrt{(kh)^2 + (lh)^2},$

$lh = 2\pi nh/B$

where B denotes the flume width and n, the diagonal cross-waves' wave number mode along the direction transverse to the flow.

Then, assuming that the wavelengths in equations (7) and (8) are both the same, they eliminate them, and the relationship of the Froude number and the mean depth is obtained as follows:

$$Fr^2 = \frac{-\alpha^2\left\{1 - \frac{2}{3}A\right\} \pm \alpha\sqrt{\frac{4}{9}A - \frac{4}{3} + \alpha^2}}{2\left\{\alpha^2 A - 1\right\}} \tag{9}$$

where $A = \left(\frac{2\pi h}{B/n}\right)^2.$

Equation (9) has a singularity at $A = 1/\alpha^2$, where the Froude number can be infinite.

The Froude number can be expressed using Manning's equation and Hey's equation respectively as follows:

$$Fr^2 = \frac{h^{1/3} I}{gN^2}, \tag{10}$$

$$Fr^2 = \left\{6.5\left(\frac{h}{3.5d_{84}}\right)^{1/4}\right\}^2 I, \tag{11}$$

where N denotes Manning's roughness coefficient; d_{84}, the grain size in cumulative 84%; and I, the bed slope. Eliminating the Froude number from equations (9), (10), and (11), the flow depth can be obtained in the case where both wavelengths are the same. Then, we can obtain the combination of the bed slope and the discharge per unit width for the generation of step-pools. Equations (9), (10), and (11) have to be calculated numerically. One of the results is nearly equivalent to the flow depth at the singularity of equation (9):

$$h = 0.192B/n. \tag{12}$$

Therefore, to generate step-pools, only equation (12) needs to be satisfied. Equations (10) and (11) are only used to calculate the values of the discharge that match the flow depth derived from equation (12) (Hasegawa & Kanbayashi, 1996).

3. EXPERIMENTAL METHODS

We used a glass-walled recirculating flume 10 m long, 40 cm deep, and 30 cm wide, with adjustable slope in Hokkaido University for the experiments. The discharge of water was measured by the weir mounted at the upstream end. Well-sorted quarts fine sand, whose mean diameter is 0.18 mm, was used. When antidunes were being formed, additional sand and silicon carbide abrasives were added from the top of the flume in a manner similar to sediment rain, so that the bed surface gradually aggraded. The abrasives made the internal structures more distinct. After the bed surface aggraded to a height of approximately 5 cm, the tailgate was suddenly closed and the pump was switched off. As a result, the water level increased and the flow stopped so that very little bed-deformation could occur. The flume then be drained very slowly without altering the bed features.

Sedimentary structures in the section parallel to the flow were observed and traced through the glass windows. Then, the sediments were cut to make sections perpendicular to the flow at intervals of 1 cm to observe the sedimentary structures.

4. RESULTS

4.1 Formation of 3D antidunes

Figure 1 shows the genetic condition of 3D antidunes for fine sand (diameter: 0.2 mm) in terms of the relationship between the bed slope and the discharge per unit width according to the equations mentioned in Chapter 2.2. n denotes the wave number mode along the direction transverse to the flow. When the flow discharge is low, two or three trains of 3D antidunes are formed. The conditions used in this study are listed in Table 1, and they are indicated by the four points shown in Figure 1. Although 3D antidunes occur at any condition on the lines, we selected these points near the boundary of the super-critical flow, i.e., where the Froude number is near unity, because it is easy to treat them.

Table 1. Experimental conditions used in this study

Run	Discharge q (m^3/s/m)	Slope I	Depth h (cm)	Velocity U (m/s)	Froude No. Fr
1	0.039	0.00945	4.6	0.87	1.29
2	0.043	0.01158	3.02	1.43	2.63
3	0.043	0.01158	3.61	1.20	2.02
4	0.045	0.01138	4.18	1.09	1.71

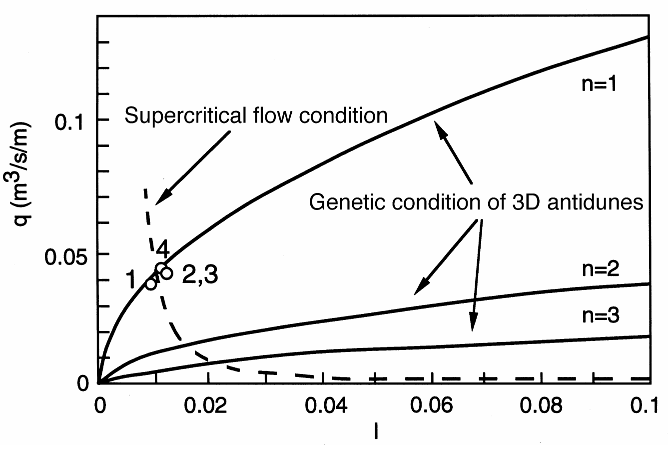

Figure 1. Genetic condition for 3D antidunes of fine sand (diameter: 0.2 mm) in terms of the relationship between the bed slope and the discharge per unit width. See the equations in Chapter 2.2. n denotes the wavenumber mode of the diagonal cross-waves in the transverse direction to the flow. The four points indicate the conditions used in this study.

3D surface waves and antidunes are formed by the following process (Figure 2). First, 2D antidunes were formed (Fig. 2a), and they triggered the water surface diagonal waves. When the wavelengths of both the antidunes and the surface diagonal waves are the same, both waves interfere and make the bed surface 3D. This leads to the formation of 3D water surface waves (Fig. 2b). Then, the 3D water surface waves become steeper, and project outward (called as "rooster-tails"; Fig. 2c). By this time, the bed waves already begin to diminish. Then, the projecting surface waves break, waves on the bed and water surface flatten away, and 2D antidunes and in-phase surface waves begin developing again.

Under these conditions, 3D and 2D antidunes occur alternately. Although 3D antidunes are ephemeral, if we can stop the flow in time, the 3D mound-like, hummocky geometry remains on the bed (Fig. 3). Figure 3 shows an oblique view of 3D antidunes after draining. The gently undulated, three dimensional, round hummocks and swales are prominent. The wavelength and wave height of the antidunes is approximately 50 cm and 2 cm, respectively. This is the case for $n=1$ and thus the three-dimensionality was not caused by the friction of the walls.

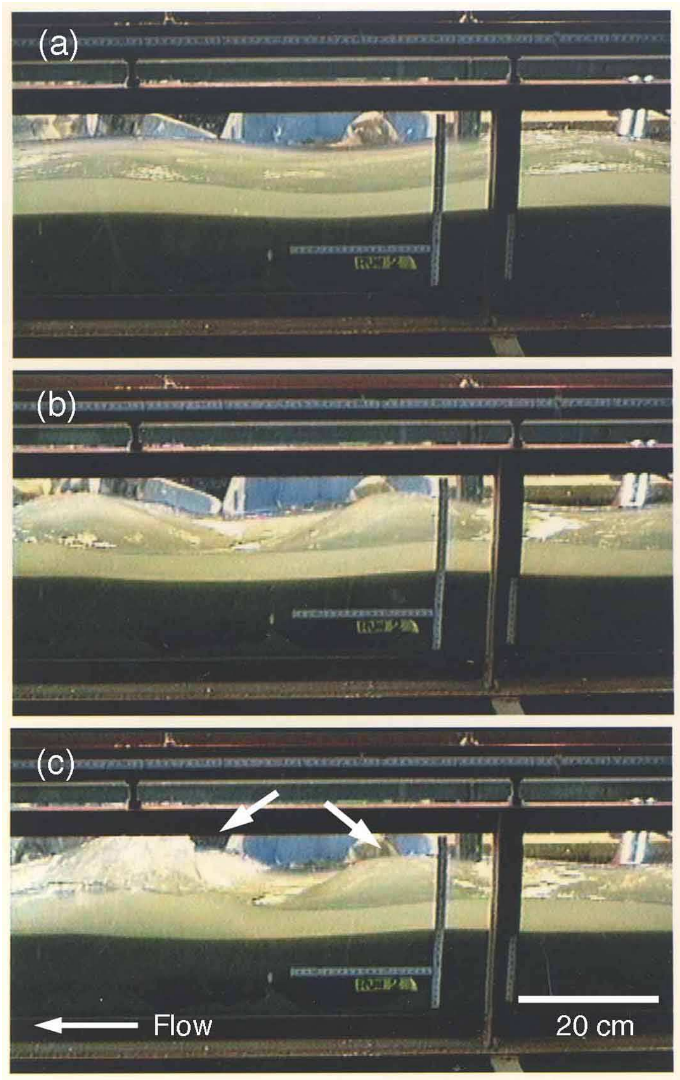

Figure 2. Movie images showing the formation of 3D antidunes. See text in detail.

4.2 Internal sedimentary structures

The sedimentary structures including 3D antidunes remain in the sediments with the additional supply of sand (Fig. 4). Figure 4a shows a line drawing of the internal structure of the 3D antidunes parallel to the flow, as traced through the glass sidewalls. The bed surface is gently undulating, and it is almost symmetrical. The wavelength and wave height are approximately 50 cm and 1–2 cm, respectively. Almost symmetrical shallow lens-like structures are found to be remarkably dominant. The wavelength of the lenses is shorter than that of the surface waves (distribution: 15–30 cm and wave height: 0.5–3 cm).

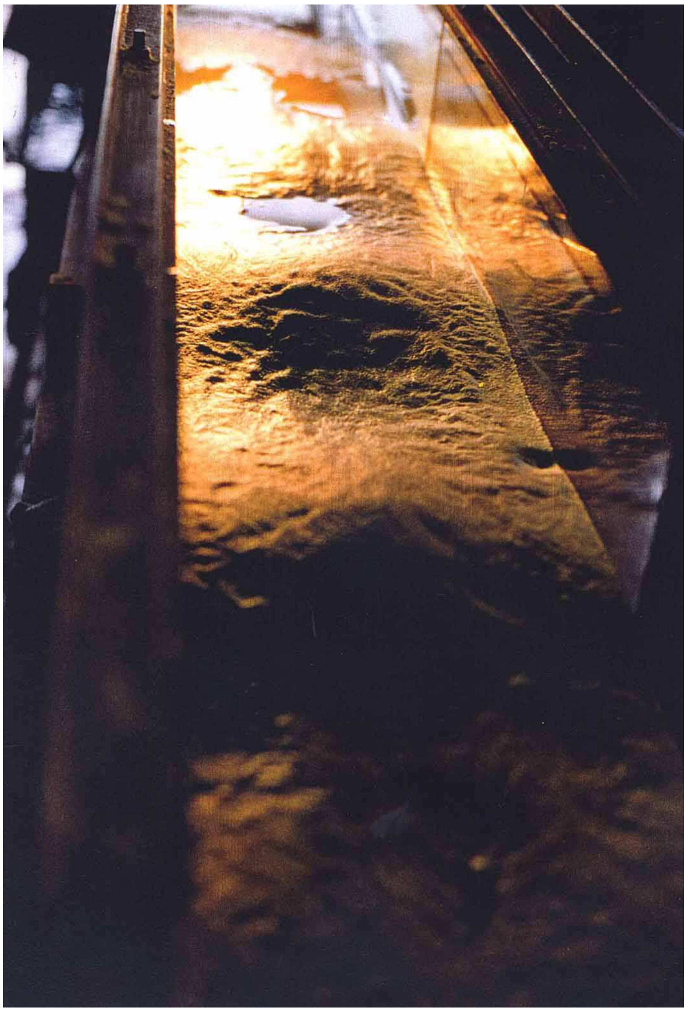

Figure 3. Oblique view of 3D antidunes after draining. The width of the flume is 30 cm. The flow was along a direction away from the viewer. Gently undulated, 3D, round hummocks and swales are prominent. The wavelength and wave height of the antidunes is approximately 50 cm and 2 cm, respectively. This is the case for $n = 1$.

The lenses are truncated by the next upstream-side lenses in most cases. The bases of the lenses are erosional surfaces. These erosional surfaces are mantled by smaller lenses. The inside of each lens appears massive in most cases, although upstream dipping foreset-like structures are rarely observed in some lenses. In addition, a gently dipping convex-upward lamination is observed. This lamination occurs as a result of the preservation of antidune crests. The angle-of-repose avalanche cross-lamination such as is typical of ripple lamination is absent. These structures appear similar to hummocky and swaley cross-stratification, which are generated by waves or combined flows.

The sedimentary structures in the section perpendicular to the flow (Fig. 4b) are also undulating wavy laminated ones similar to those in the section parallel to the flow. Shallow lens-like structures whose bases are erosional surface are characteristic. Although gently dipping concave-upward lamination dominantly occurs, convex-upward lamination is occasionally observed as well. The characteristic features of these transverse sections are shallow lens-like structures sandwiched between almost planar (slightly wavy) laminations. This could be attributed to the alternate occurrence of 3D antidunes, plane beds, and 2D antidunes.

(a)

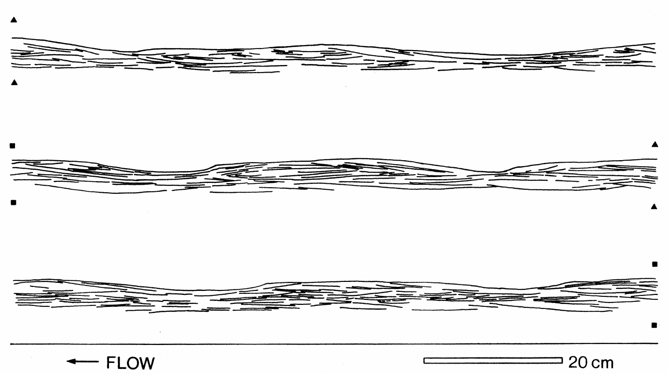

(b)

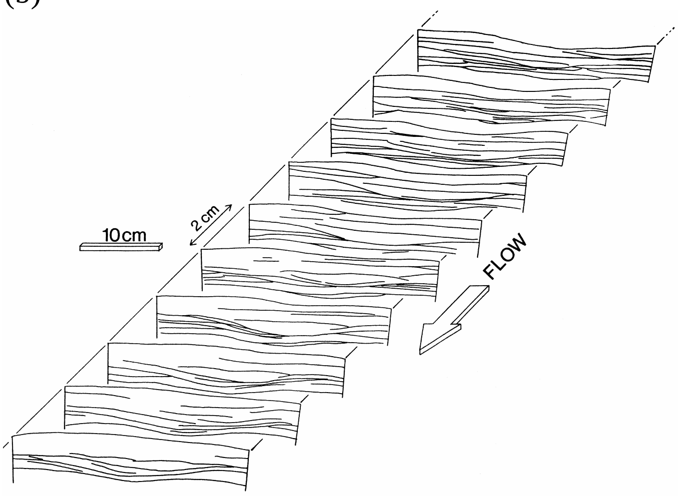

Figure 4. (a) Flow-parallel line diagrams of the internal sedimentary structure of 3D antidunes, as traced through the glass sidewalls. The scale is 20 cm. The flow was from the right to the left. (b) Flow-perpendicular line diagrams, as traced from the photographs of successive sections. The scale is 20 cm. The flow was along a direction heading out of the diagram. Undulating wavy laminations and shallow lens-like structures whose bases are erosional surface are characteristic. Although gently dipping concave-upward lamination occurs dominantly, convex-upward lamination is occasionally observed as well. The

shallow lens-like structures are sandwiched between almost planar (slightly wavy) laminations.

5. DISCUSSION

Hydraulic conditions in this study are consistent with the previously known antidune genetic conditions described in Chapter 2.1, and the relationship between the antidune wavelength and the averaged flow velocity is also consistent with the former studies. Thus, the 3D antidunes generated in this study are not peculiar ones but fall into well known antidune range. 3D antidunes have been reported in the gravel beds in modern rivers (e.g., Shaw & Kellerhals, 1977; Carling & Breakspear, 2007). This may be because once gravel forms mound structures, it aggregates and then cannot be dislodged by waning flows. On the contrary, only small numbers of 3D antidunes have been reported on sand beds from rock records (Rust & Gibling, 1990; Prave & Duke, 1990; Masuda et al., 1993; Collinson et al., 2006). To the best of our knowledge, no "preserved" 3D antidune has been reported in a sand bed from either modern rivers or from experiments. This study showed that 3D-antidune beds can be preserved if the genetic conditions are satisfied, and if the timing and manner of flow deceleration is suitable for preserving the bed configuration. Despite their low preservation potential, sandy 3D antidunes may have remained unnoticed, as pointed out by Rust & Gibling (1990).

As compared to the surface configuration, internal sedimentary structures can be preserved more easily if bed accumulation occurs. The internal sedimentary structures obtained in this study are essentially identical to those of 2D antidunes (Yokokawa et al., 1999; Alexander et al., 2001). In the sections transverse to the flow, the combination of shallow lens-like structures and almost planar (slightly wavy) laminations are characteristic in this study. This reflects the periodic occurrence of 2D antidunes, 3D antidunes, and plane beds, as described in Chapter 4.1. Although further studies are required to reveal the relationship between the bed-aggradation rates and the preserved sedimentary structures, the combinations of the cross stratification of shallow lens-like antidunes and planar (slightly wavy) laminations can be preserved when the hydraulic condition described in this study remains the same for some duration, and there is adequate sediment supply and accommodation space.

Alexander et al. (2001) described that the mean laminaset length/mean antidune length is approximately 0.5 and the maximum laminaset thickness/mean formative antidune height is around 0.6 based on the examples from modern environments (Langford & Bracken, 1987; Barwis & Hayes, 1985), and these values are in good agreement with their experimental observations. In this study, the laminaset length and height is also approximately half of that of the antidunes preserved on the bed surface. Although more data should be examined to refine these relationships, it appears that the geometry of lenticular laminasets can be used to estimate the antidune geometry, as stated by Alexander et al. (2001).

If 3D configurations are found on the bed surface (gravel or sand bed), it is highly possible that they result from the interaction between antidunes and 3D water surface waves (diagonal cross-waves). Thus, using the formula given in this study, the possible combinations of discharges and bed slopes can be estimated. Even if only sedimentary structures are found, if the diagnoses of 3D antidunes are found using the relationship between the dimensions of the laminasets and the formative antidunes, it is still possible to estimate paleo-hydraulic conditions such as the flow depth or water discharge.

6. CONCLUSIONS

In this study, the genetic conditions of 3D gravel step-pool topographies applied to sand beds with the same conditions yield 3D antidunes on the sand bed. Step-pools are generated due to the interaction of 2D antidunes and water surface waves (diagonal cross-waves). When the wavelengths of the antidunes and the water surface waves coincide, the 2D undulation of antidunes becomes 3D. Although 3D antidunes occur alternately with 2D antidunes under these conditions, 3D mound-like antidunes and internal sedimentary structures were left behind by the additional sand supply and sudden decrease in the flow of the dammed up flume. The genetic condition is expressed as the relationship between the bed slope and the water discharge per unit width. If 3D antidune configurations are found, the paleo-hydraulic parameters can be obtained more precisely than in previous cases.

The internal sedimentary structures were also observed in detail. Shallow lens-like structures whose bases are erosional surfaces are characteristic. Although gently dipping concave-upward lamination occurs dominantly, convex-upward lamination is occasionally observed as well. The characteristic features of flow-transverse sections are that shallow lens-like structures are sandwiched between almost planar (slightly wavy) laminations. This could be attributed to the alternate occurrence of 3D antidunes, plane beds, and 2D antidunes. The laminaset length and height is approximately half of that of the antidunes preserved on the bed surface; this is consistent with previous studies. Although more data should be examined to refine these relationships, it appears that the geometry of lenticular laminasets can be used to estimate the antidune geometry. Thus, if only sedimentary structures and the diagnoses of 3D antidunes are found, it will still be possible to estimate paleo-hydraulic parameters such as the flow depth and water discharge.

ACKNOWLEDGEMENTS

This experiment was supported by the Grant-in-Aid for Scientific Research (c)(07650585) for KH. We would like to thank Prof. Fujio Masuda of Doshisha University, and Dr. Hajime Naruse of Chiba University for their valuable discussions.

REFERENCES

Alexander, J. & Fielding, C.R. 1997. Gravel antidunes in the tropical Burdekin River, Queensland, Australia. *Sedimentology* 44: 327-337.

Alexander, J., Bridge, J.S., Cheel, R.J. & Leclair, S. 2001. Bedforms and associated sedimentary structures formed under supercritical water flows over aggrading sand beds. *Sedimentology* 48: 133-152.

Allen, J.R.L. 1982, *Sedimentary Structures: Their Character and Physical Bases, Vol. 1. Developments in Sedimentology 30*, Amsterdam, Elsevier Science Publishers.

Anderson, A.G. 1953, The characteristics of sediment waves formed by flow in open channels. *Proceedings, 3rd Midwest Conference on Fluid Mechanics, 23-25 March 1953. Univ. Minesota*: 379-395.

Ashida, K., Egashira, S. & Ando, N. 1984. Generation and geometric features of Step-pool bed forms. *Kyoto Univ. Disas. Prev. Res. Inst. Annuals* 27 (B-2): 341-353. (in Japanese)

Augustinus, P.G.E.F. 1980. Actual development of the chenier coast of suriname (South America). *Sedimentary Geology* 26: 91-113.

Barwis, J.H. & Hayes, M.O. 1985. Antidunes on modern and ancient washover fans. *Journal of Sedimentary Petrology* 55: 907-916.

Boguchwal, L.A. & Southard, J.B. 1990. Bed configurations in steady unidirectional water flows. Part3. Effects of temperature and gravity. *Journal of Sedimentary Perology* 60: 680-686.

Burr, D.M., Carling, P.A., Beyer, R.A. & Lancaster, N. 2004, Flood-formed dunes in Athabasca Valles, Mars: morphology, modeling, and implications. *Icarus* 171: 68-83.

Carling, P.A. & Breakspear, R.M.D. 2007. Gravel dunes and antidunes in fluvial systems. In Dohmen-Janssen, C.M. & Hulscher, S.J.M.H. (eds.), *River, Coastal and Estuarine Morphodynamics: RCEM2007*, Taylor & Francis:1015-1020.

Carling, P.A. & Shvidchenko, A.B. 2002. A consideration of the dune:antidune transition in fine gravel. *Sedimentology* 49: 1269-1282.

Collinson, J.D., Mountney, N. & Thompson, D.B. 2006. *Sedimentary Structures 3rd ed.* Hertfordshire: Terra Publishing: 130-131.

Fielding, C.R. 2006. Upper flow regime sheets, lenses and scour fills: Extending the range of architectural elements for fluvial sediment bodies. *Sedimentary Geology* 190: 227-240.

Foley, M.G. 1977, Gravel-lens formation in antidune-regime flow- A quantitative hydrodynamic indicator. *Journal of Sedimentary Petrology* 47: 738-746.

Gustavson, C.T. 1974. Sedimentation on Gravel outwash fans, Malaspina Glacier Foreland, Alaska. *Journal of Sedimentary Petrology* 44: 374-389.

Hasegawa, K., Mori, A. & Ishikawa, S. 1990. Bed topographies and sediment transport during flood in mountainous rivers. In White, W.R. (ed.), *International Conference on River Flood Hydraulics*, John Wiley & Sons.

Hasegawa, K. & Kanbayashi, S. 1996. Formation mechanism of step-pool systems in steep rivers and guide lines for the design of construction. *Journal of Hydroscience and Hydraulic Engineering* 40: 893-900. (in Japanese with English abstract)

Hayashi, T. 1970. Formation of dunes and antidunes in open channels. *Proc. ASCE, Jour. of Hydraulics Div.* 96, (HY2): 431-439.

Kennedy, J.F. 1961. Stationary waves and antidunes in alluvial channels. *W.M.Keck Lab. of Hydraulics and Water Resources, California Institute of Technology, Report.* KH-R-2, 146p.

Kennedy, J.F. 1963. The mechanics of dunes and antidunes in erodible-bed channels. *Journal of Fluid Mechanics* 16: 521-544.

Kennedy, J.F. 1969. The formation of sediment ripples, dunes, and antidunes. *Annual Review of Fluid Mechanics* 1: 147-168.

Langford, R. & Bracken, B. 1987. Medano creek, Colorado, a model for upper-regime fluvial deposition. *Journal of Sedimentary Petorology*, 57: 863-870.

Masuda, F., Yokokawa, M. & Sakamoto, T. 1993. HCS mimics in Pleistocene, tidal deposits of the Shimosa Group and flood deposits of the Osaka Group, Japan. *Journal of Sedimentological Society of Japan* 39: 27-34. (in Japanese with English abstract)

Parker, G. 2004. *1D Sediment Transport Morphodynamics with Applications to Rivers and Turbidity Currents*. Chap. 8. Fluvial Bedforms. http://cee.uiuc.edu/people/parkerg/morphodynamics_e-book.htm

Prave, A.R. & Duke, W.L. 1990. Small-scale hummocky cross-stratification in turbidites: a form of antidune stratification? *Sedimentology* 37: 531-539.

Rust, B.R. & Gibling, D. A. 1990. Three-dimensional antidunes as HCS mimics in a fluvial Sandstone: the Pennsylvanian South Bar Formation near Sydney, Nova Scotia. *Journal of Sedimentary Petrology* 60: 540-548.

Schmincke, H.-U., Fosher, R.V. & Waters, A.C. 1973. Antidune and chute and pool structures in the base surge deposits of the Laacher See area, Germany. *Sedimentology* 20: 553-574.

Shaw, J. & Kellerhals, R. 1977. Paleohydraulic interpretation of antidune bedforms with applications to antidunes in gravel. *Journal of Sedimentary Petrology* 47: 257-266.

Whittaker, J.G. & Jaeggi, M.N.R. 1982. Origin of Step-pool systems in mountain streams. *Journal of Hydraulic Division, Proceedins of ASCE 108 (HY6)*: 758-773.

Yokokawa, M., Masuda, F., Sakai, T., Endo, N. & Kubo Y. 1999. Sedimentary structures generated in upper-flow-regime with sediment supply. In Saito, Y. (ed.) *Proc. of International Workshop on Sediment Transport and Storage in Coastal Sea-Ocean Systems.* STA(JIS-TEC) & Geol. Surv. Japan, Tsukuba, Japan: 409-414.